Phase regeneration for polarization-division multiplexed signals based on vector dual-pump nondegenerate phase sensitive amplification

Weili Yang, Yu Yu,* Mengyuan Ye, Guanyu Chen, Chi Zhang, and Xinliang Zhang

Wuhan National Laboratory for Optoelectronics, Huazhong University of Science and Technology, Wuhan 430074, China

yuyu@mail.hust.edu.cn

Abstract: The polarization-division multiplexing (PDM) technology is a practical method to double the transmission capacity, and the corresponding phase regeneration (PR) for PDM signals is meaningful and necessary to extend the transmission distance and increase the transparency for the phase-encoded PDM system. Those reported PDM PR schemes either utilized polarization-diversity technique or required special PDM format. In order to overcome these issues, the PR for the PDM phase-modulated signals is proposed and theoretically demonstrated in this paper, based on the vector dual-pump nondegenerate phase sensitive amplification (PSA). The theoretical model is established and the detailed characteristics are investigated to optimize the PR performance. Results show an obvious phase squeezing for the degraded 80 Gbit/s PDM differential phase-shift keying (DPSK) signals, and the error vector magnitude (EVM) of the regenerated signals on dual polarization states can be improved from 22.58% and 21.39% to 4.57% and 4.63%, respectively. Furthermore, the applicability of the proposed scheme for PDM quaternary-phase shift keying (QPSK) signals is investigated. The proposed scheme can be useful and promising in current PDM based coherent fiber-optic communication.

OCIS codes: (060.4230) Multiplexing; (070.4340) Nonlinear optical signal processing; (190.4380) Nonlinear optics, four-wave mixing; (190.4975) Parametric processes.

References and links

1. K. Kikuchi, "Analyses of wavelength- and polarization-division multiplexed transmission characteristics of optical quadrature-amplitude-modulation signals," Opt. Express **19**(19), 17985–17995 (2011).
2. J. Sakaguchi, B. J. Puttnam, W. Klaus, Y. Awaji, N. Wada, A. Kanno, T. Kawanishi, K. Imamura, H. Inaba, K. Mukasa, R. Sugizaki, T. Kobayashi, and M. Watanabe, "19-core fiber transmission of 19x100x172-Gb/s SDM-WDM-PDM-QPSK signals at 305Tb/s," *in Proc. OFC* (2012), Paper PDP5C.1.
3. K. Croussore and G. Li, "Phase regeneration of NRZ-DPSK signals based on symmetric-pump phase-sensitive amplification," IEEE Photon. Technol. Lett. **19**(11), 864–866 (2007).
4. A. Fragkos, A. Bogris, and D. Syvridis, "All-optical regeneration based on phase-sensitive nondegenerate four-wave mixing in optical fibers," IEEE Photon. Technol. Lett. **22**(24), 1826–1828 (2010).
5. R. Slavik, F. Parmigiani, J. Kakande, C. Lundström, M. Sjödin, P. A. Andrekson, R. Weerasuriya, S. Sygletos, A. D. Ellis, L. Grüner-Nielsen, D. Jakobsen, S. Herstrøm, R. Phelan, J. O'Gorman, A. Bogris, D. Syvridis, S. Dasgupta, P. Petropoulos, and D. J. Richardson, "All-optical phase and amplitude regenerator for next-generation telecommunications systems," Nat. Photonics **4**(10), 690–695 (2010).
6. P. Frascella, S. Sygletos, F. C. G. Gunning, R. Weerasuriya, L. Grüner-Nielsen, R. Phelan, J. O'Gorman, and A. D. Ellis, "DPSK signal regeneration with a dual-pump nondegenerate phase-sensitive amplifier," IEEE Photon. Technol. Lett. **23**(8), 516–518 (2011).
7. M. A. Ettabib, F. Parmigiani, X. Feng, L. Jones, J. Kakande, R. Slavík, F. Poletti, G. M. Ponzo, J. Shi, M. N. Petrovich, W. H. Loh, P. Petropoulos, and D. J. Richardson, "Phase regeneration of DPSK signals in a highly nonlinear lead-silicate W-type fiber," Opt. Express **20**(24), 27419–27424 (2012).
8. S. Sygletos, P. Frascella, S. K. Ibrahim, L. Grüner-Nielsen, R. Phelan, J. O'Gorman, and A. D. Ellis, "A practical phase sensitive amplification scheme for two channel phase regeneration," Opt. Express **19**(26), B938–B945 (2011).

#225809 - $15.00 USD Received 27 Oct 2014; revised 11 Dec 2014; accepted 6 Jan 2015; published 26 Jan 2015

9. S. Sygletos, M. J. Power, F. C. G. Gunning, R. P. Webb, R. J. Manning, and A. D. Ellis, "Simultaneous dual channel phase regeneration in SOAs," *in Proc. ECOC* (2012), Paper Tu.1.A.2.
10. K. Inoue and S. Okazaki, "Phase-sensitive amplification in fiber-loop for QPSK signal regeneration," *in Proc. CLEO* (2013), Paper JW2A.23.
11. J. Kakande, A. Bogris, R. Slavík, F. Parmigiani, D. Syvridis, P. Petropoulos, D. Syvridis, M. Sköld, M. Westlund, P. Petropoulos, and D. J. Richardson, "QPSK phase and amplitude regeneration at 56 Gbaud in a novel idler-free non-degenerate phase sensitive amplifier," *in Proc. OFC* (2011), Paper OMT4.
12. J. Y. Yang, Y. Akasaka, and M. Sekiya, "Optical QPSK regeneration using dual-pump degenerate phase-sensitive amplification," *in Proc. OECC* (2012), 907–908.
13. T. Richter, R. Elschner, and C. Schubert, "QAM phase-regeneration in a phase-sensitive fiber-amplifier," *in Proc. ECOC* (2013), Paper We.3.A.2.
14. A. Bogris and D. Syvridis, "All-optical signal processing for 16-QAM using four-level optical phase quantizers based on phase sensitive amplifiers," *in Proc. ECOC* (2013), Paper We.3.A.6.
15. B. Stiller, G. Onishchukov, B. Schmauss, and G. Leuchs, "Phase regeneration of a star-8QAM signal in a phase-sensitive amplifier with conjugated pumps," Opt. Express **22**(1), 1028–1035 (2014).
16. T. Richter, R. Elschner, and C. Schubert, "Phase-regeneration of 2ASK-BPSK in a one-mode phase-sensitive amplifier," *in Proc. Photonics Society Summer Topical Meeting Series* (2013), 157–158.
17. T. Umeki, O. Tadanaga, M. Asobe, Y. Miyamoto, and H. Takenouchi, "First demonstration of high-order QAM signal amplification in PPLN-based phase sensitive amplifier," *in Proc. ECOC*(2013), Paper pd1-c-5.
18. J. Y. Yang, M. Ziyadi, Y. Akasaka, S. Khaleghi, M. R. Chitgarha, J. Touch, and M. Sekiya, "Investigation of polarization-insensitive phase regeneration using polarization-diversity phase-sensitive amplifier," *in Proc. ECOC*(2013), Paper P.3.9.
19. C. McKinstrie and S. Radic, "Phase-sensitive amplification in a fiber," Opt. Express **12**(20), 4973–4979 (2004).
20. A. Lorences-Riesgo, F. Chiarello, C. Lundström, M. Karlsson, and P. A. Andrekson, "Experimental analysis of degenerate vector phase-sensitive amplification," Opt. Express **22**(18), 21889–21902 (2014).
21. A. L. Riesgo, C. Lundström, F. Chiarello, M. Karlsson, and P. A. Andrekson, "Phase-sensitive amplification and regeneration of dual-polarization BPSK without polarization diversity," in *Proc. ECOC* (2014), Paper Tu.1.4.3.
22. C. Lundström, Z. Tong, M. Karlsson, and P. A. Andrekson, "Phase-to-phase and phase-to-amplitude transfer characteristics of a nondegenerate-idler phase-sensitive amplifier," Opt. Lett. **36**(22), 4356–4358 (2011).
23. F. Da Ros, D. Vukovic, A. Gajda, K. Dalgaard, L. Zimmermann, B. Tillack, M. Galili, K. Petermann, and C. Peucheret, "Phase regeneration of DPSK signals in a silicon waveguide with reverse-biased p-i-n junction," Opt. Express **22**(5), 5029–5036 (2014).
24. R. Phelan, B. Kelly, J. O'Carroll, C. Herbert, A. Duke, and J. O'Gorman, "-40° C< T < C mode-hop-free operation of uncooled AlGaInAs-MQW discrete-mode laser diode with emission at 1.3um," Electron. Lett. **45**(1), 43 (2009).
25. Q. Lin and G. P. Agrawal, "Vector theory of four-wave mixing: polarization effects in fiber-optic parametric amplifiers," J. Opt. Soc. Am. B **21**(6), 1216–1224 (2004).
26. R. Tang, J. Lasri, P. S. Devgan, V. Grigoryan, P. Kumar, and M. Vasilyev, "Gain characteristics of a frequency nondegenerate phase-sensitive fiber-optic parametric amplifier with phase self-stabilized input," Opt. Express **13**(26), 10483–10493 (2005).
27. C. Lundström, B. Corcoran, M. Karlsson, and P. A. Andrekson, "Phase and amplitude characteristics of a phase-sensitive amplifier operating in gain saturation," Opt. Express **20**(19), 21400–21412 (2012).
28. P. A. Andrekson, C. Lundström, and Z. Tong, "Phase-sensitive fiber-optic parametric amplifiers and their applications," in Proc. ECOC. Paper. We.6. E.1 (2010).
29. R. Schmogrow, B. Nebendahl, M. Winter, A. Josten, D. Hillerkuss, S. Koenig, J. Meyer, M. Dreschmann, M. Huebner, C. Koos, J. Becker, W. Freude, and J. Leuthold, "error vector magnitude as a performance measure for advanced modulation formats," IEEE Photon. Technol. Lett. **24**(1), 61–63 (2012).
30. J. Kakande, R. Slavik, F. Parmigiani, A. Bogris, D. Syvridis, L. Grüner-Nielsen, R. Phelan, P. Petropoulos, and D. J. Richardson, "Multilevel quantization of optical phase in a novel coherent parametric mixer architecture," Nat. Photonics **5**(12), 748–752 (2011).

1. Introduction

To meet the exponentially growing demand of the communication capacity, the optical communication networks with high spectral efficiency (SE) are urgently desired. Besides the optical time-division multiplexing (OTDM), the wavelength-division multiplexing (WDM) and the space-division multiplexing (SDM) technologies, the polarization-division multiplexing (PDM) is also an effective method to double the SE by transmitting two independent signals utilizing two orthogonal polarization states on a same wavelength [1]. As a result, the multi-dimensional multiplexing is becoming a feasible and successful approach to update the record transmission capacity [2]. On the other hand, all-optical phase regeneration (PR) is widely regarded as a key technology to extend the transmission distance and increase the transparency in the phase-encoded optical communication systems, in which the nonlinear

#225809 - $15.00 USD Received 27 Oct 2014; revised 11 Dec 2014; accepted 6 Jan 2015; published 26 Jan 2015

phase noise (PN) is a main limiting factor. Thus, a regenerator capable of removing the PN is highly desired in both the direct detection and coherent communication. During the past decades, the phase sensitive amplification (PSA) has attracted continuous attention because of the ability to remove the PN of the phase-modulated signals, including the differential phase-shift keying (DPSK) [3–9], the quaternary-phase shift keying (QPSK) [10–12] and the higher-order quadrature amplitude modulation (QAM) signals [13–17].

The PSA is intrinsically a four wave mixing (FWM) process, excepting that all the waves involved in the PSA should be prepared before being injected into the nonlinear medium. PSA is divided into scalar and vector types, depending on the polarization states of the interacting waves. Either type can be subdivided into dual-pump degenerate, dual-pump nondegenerate and single-pump nondegenerate PSA. Most of the reported PR schemes were performed with the scalar PSA in the nonlinear device. Limited by the same polarization states of the interacting waves in the scalar PSA, the scalar scheme is not capable of the PDM PR, unless utilizing the polarization-diversity set-up [18]. By contrast, the vector scheme utilizing two orthogonal pumps, has been also theoretically proposed and experimentally demonstrated to have the potential for the PR of single polarized signal [19, 20]. Compared to the scalar PSA, the vector scheme has lower phase sensitive gain (PSG) with the same input conditions excepting for the polarization states of the waves, resulting in a slightly worse regenerative performance. Even so, the vector PSA is feasible for the PDM signal regeneration. Recently, a successful demonstration for the PR of PDM binary phase-shift keying (BPSK) signals utilizing vector dual-pump degenerate PSA was firstly presented [21]. However, owing to the indistinguishable wavelengths of signal and idler involving the PSA, the PDM BPSK format is limited to be a conjugated pair of QPSK. One of the BPSK signals is phase rotated by $\pi/2$. The phase rotation may be implemented with additional phase modulator (PM) or optical processor in practice. Therefore, a phase regenerator with respect to conventional PDM format is urgently required in the PDM communication system, and a theoretical analysis and characterization for the phase regenerator is also essential in order to evaluate the regenerative performance for PDM signals.

In this paper, we thus propose and theoretically demonstrate the simultaneous PDM PR scheme for phase-modulated signals based on the vector PSA. A theoretical model for the PDM PR is established, and the key parameters in the PR are investigated. The PDM signals are involved into two different vector PSA processes, in which the vector dual-pump nondegenerate configuration is employed. In order to optimize the DPSK PR performance, a detailed simulation in view of several typical input parameters, including the signal-to-idler power ratio, the total pump power, the signal power, and the linear wavenumber mismatch factor related to the PSA processes, is presented. For demonstration, the PR for 80 Gbit/s PDM return-to-zero DPSK (RZ-DPSK) signals is realized by simulation based on a high nonlinear fiber (HNLF). The error vector magnitudes (EVMs) of the regenerated signal on dual polarization states are improved from 22.58% and 21.39% to 4.57% and 4.63%, respectively. Furthermore, the applicability of the proposed scheme for PDM-QPSK signal is investigated using the proposed scheme. The scheme is potential in the fiber optic communication system utilizing the PDM technique.

#225809 - $15.00 USD Received 27 Oct 2014; revised 11 Dec 2014; accepted 6 Jan 2015; published 26 Jan 2015

2. The PR model and analysis based on vector PSA

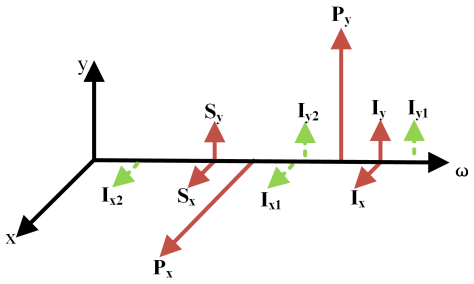

Fig. 1. Polarization and frequency diagram for vector dual-pump nondegenerate PSA processes for PDM PR. ***P***: pump; ***S***: signal; ***I***: idler. x and y denote two orthogonal polarization states. Red solid line: launched wave; green dash line: generated line.

The configuration of the vector dual-pump nondegenerate PSA for PDM PR is shown in Fig. 1. x and y denote two orthogonal polarization states. The red solid line represents the launched wave, and the green dash line represents the generated wave. The PDM signals S_x and S_y, the orthogonal pumps P_x and P_y, and the idlers I_x and I_y, are involved in two different vector PSA processes, i.e. S_x - P_x - P_y - I_y and S_y - P_x - P_y - I_x, respectively. The orthogonal pumps, P_x and P_y, are shared. In each PSA process, the PDM component and the corresponding idler are respectively aligned to the orthogonal pumps.

For the regeneration of PDM DPSK signals, the relative phase difference relationship among the interacting waves in each PSA process should satisfy the quantization of two-phase state condition, which can be obtained when the idlers carry the same information as the corresponding signals [22]. Here, a possible solution to achieve the needed idlers is presented as follows.

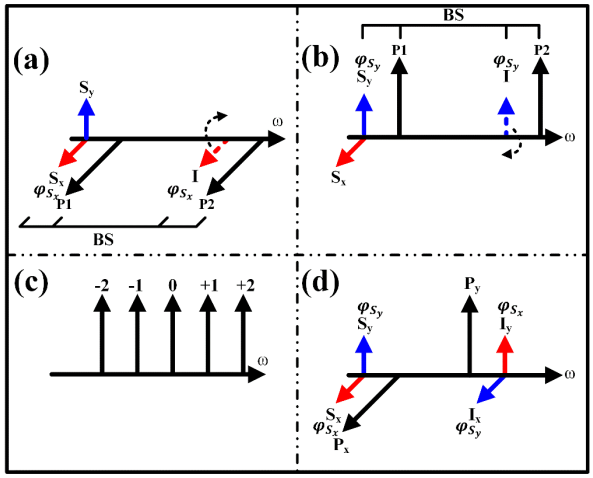

Fig. 2. Operation principle. (a) vector PIA process to generate the idler carrying the same phase information as S_x; (b) vector PIA process to generate the idler carrying the same phase information as S_y; (c) frequency comb and (d) input of vector PSA processes. Red line: the PIA/PSA process S_x participates *in*; blue line: the PIA/PSA process S_y participates in*;* black line: pumps. Solid line: input wave; dash line: generated wave. *S*: signal; *I*: idler; *P*: pump. BS: Bragg scattering.

The operation principle is shown in Fig. 2. The idlers are separately achieved based on two scalar phase insensitive amplifiers (PIAs) of Bragg scattering (BS) type, with the spectra shown in Fig. 2(a)–2(b). The red and blue lines are utilized to distinguish the PIA/PSA process each PDM component participating in. The black lines represent the pumps. The solid

#225809 - $15.00 USD Received 27 Oct 2014; revised 11 Dec 2014; accepted 6 Jan 2015; published 26 Jan 2015

and dash lines are to distinguish the input and generated waves, respectively. In each PIA process, by matching the polarization state of the pumps with that of each PDM component, the idlers are separately generated and consequently launched into the nonlinear medium for PSA processes. Various devices can be utilized for the FWM processes, here the HNLF is employed [5, 8, 16, 23]. The pumps involved in each PIA process are achieved with 3 steps: (1) A frequency comb is generated, with the spectrum shown in Fig. 2(c). The numbers (i.e. 0, ± 1, ± 2) shown in the spectrum are utilized to distinguish each comb. The frequency spacing between the adjacent combs is $\Delta\omega$. A continuous wave (CW) laser, which is injection-locked (IL) by one tributary of the input PDM signals, is utilized as the carrier of the frequency comb [24]. (2) The ± 2 levels of the frequency comb are then filtered by an optical processer (opt. proc.); (3) The filtered ± 2 level combs are divided into two paths to respectively participate in each PIA process. A polarization controller (PC) on each path may be needed to rotate the polarization of the combs, thus make their polarization states coincident with each PDM component. As the generated idlers have the same polarizations as the corresponding signals (Fig. 2(a)–2(b)), PCs are needed to rotate polarization states of the idlers for the next vector PSA processes.

The pumps utilized in the PSA processes are achieved with the similar method as aforementioned. The difference is that the −2 and 0 level combs are chosen as the pumps, considering the frequency locations of the signals and idlers. A PC before a polarization-maintaining fiber (PMF) enables the possibility of obtaining orthogonal pumps [20].

Then all the waves (i.e. the PDM signals, the idlers and the orthogonal pumps), with the spectrum shown in Fig. 2(d), are combined together to launch into the HNLF for PSA processing. The waves before being combined together propagate in different paths, thus polarization tracking and phase locked loops may be required to stabilize temporal drifts for good regenerative performance.

For the PSA process, the stationary phase stability among the interacting waves is needed. In the proposed scheme, different pumps are utilized in the PIA and PSA processes, the pumps phase-locked to each other are obtained by the frequency comb. The idlers are generated by the PIA processes, resulting in the phase of the idlers automatically locked to the signals. The carrier of the frequency comb is achieved by the IL process, thus ensuring all the pumps phase locked to the signal carrier. Consequently, based on the above processing, all the waves launched into the HNLF are phase locked, and the idlers carry the needed phase information. Besides, the pumps and idlers are generated and phase-locked locally, enabling black-box operation. In our opinion, due to the inherent property of polarization multiplexing, it is reasonable that the possible scheme for PDM signals will be more complex.

In order to theoretically investigate the PR performance based on the vector dual-pump nondegenerate PSA, the nonlinear transmission theory considering the optical Kerr nonlinear effects is used here. The vector FWM has a nonlinear coefficient which is 2/3 of that of the scalar single-pump FWM. Meanwhile, the XPM between the cross-polarized waves has a nonlinear coefficient which is 1/3 of that of the XPM between the co-polarized waves [25]. The stimulated Brillouin scattering (SBS) effect is ignored. Supposing the PDM signals S_x and S_y, the orthogonal pumps P_x and P_y, and the corresponding idlers I_x and I_y, which have been prepared in advance, are launched into the HNLF for PSA, the complex amplitude equations of the 10 waves shown in Fig. 1 can be described as follows:

$$\frac{dE_i}{dz} = i\gamma\left[\left|E_i\right|^2 + 2\left(\sum\left|E_j\right|^2 + \frac{1}{3}\sum\left|E_k\right|^2\right)\right]E_i + \left(\sum\frac{2}{3}i\gamma E_a E_b E_c^* e^{i\Delta\beta_{a,b,i,c}z} + \sum i\gamma E_p^2 E_q^* e^{i\Delta\beta_{p,p,i,q}z}\right) \tag{1}$$

where $\omega_a + \omega_b = \omega_c + \omega_i$ and $2\omega_p = \omega_i + \omega_q$ represent the vector PSA and the scalar single-pump FWM processes, respectively. ω is the wave frequency. The HNLF used here is lossless, polarization-maintaining and has no birefringence. The stimulated Brillouin

#225809 - $15.00 USD Received 27 Oct 2014; revised 11 Dec 2014; accepted 6 Jan 2015; published 26 Jan 2015

scattering (SBS) effect is also ignored. In the equations, besides two vector PSA processes, 4 scalar phase insensitive FWM processes between the signal/idler and the co-polarized pump, e.g. S_x-P_x-I_{x1}, are also taken into account. As the four scalar processes have high FWM efficiency, and may result in the regeneration crosstalk of the PDM signals, they are included to examine the influence on the PDM regeneration. Other FWM processes, which may be unavoidable in practice and affect the regeneration performance, are ignored because of lower FWM efficiency [26, 27]. Moreover, the processing will not influence the feasibility demonstration of the proposed scheme. To be noted that in order to avoid the possible crosstalk induced by the high-order FWM processes, the frequency-spacing between the pumps should be different from that between the signal carrier and the low-frequency pump.

Other parameters appear in the equation are: $\Delta\beta_{a,b,i,c} = \beta_a + \beta_b - \beta_i - \beta_c$ and β_i are the linear wavenumber mismatching factor and propagation constant, respectively. Subscripts *a*, *b*, *c*, *i* represent different waves. $E_i(z) = \sqrt{P_i(z)}e^{i\phi_i(z)}$ is the complex amplitude, $P_i(z)$ and $\phi_i(z)$ are the power and phase of the wave at z along the HNLF, γ is the nonlinear coefficient of the HNLF, and superscript $*$ is the conjugation operation.

The PSG can be utilized to assess the phase regenerative ability of the PSA, it is defined as the difference between the maximum and minimum gain of the PSA. Taking the S_x for example, the maximum and minimum gain of PSA can be achieved under the relative phase difference condition of $\varphi_{S_x} + \varphi_{I_y} - \varphi_{P_x} - \varphi_{P_y} = \pi/2$ and $\varphi_{S_x} + \varphi_{I_y} - \varphi_{P_x} - \varphi_{P_y} = 3\pi/2$, respectively. Solving the complex amplitude equations numerically, the evolution of each wave can be achieved and the signal PSG can be subsequently calculated. For a given HNLF, several input parameters may influence the PSG, including the signal-to-idler power ratio σ, the total pump power P_{pumps}, the Δβ related to the PSA processes, and the signal power P_{signal}. In the following part, in order to better regenerate the degraded signals, the PSG is characterized by optimizing these aforementioned parameters.

3. Simulations and discussion

3.1. PSG characterization

For the regeneration of DPSK signals, a large PSG in the small-signal case should be ensured to achieve the step-like phase transfer function [3, 5, 28]. In the calculation, the HNLF is 300 m long with a zero dispersion wavelength at 1550nm, a dispersion slope of 0.03 ps/nm^2/km, a four-order dispersion coefficient of -2.48×10^{-4} ps^4/km and a nonlinear coefficient of 15 /W/km. At the input of the HNLF, two continuous waves (CWs) with identical power at 1547 and 1553 nm are employed as the orthogonal pumps. Another wave at 1544.5 nm with identical power of −25 dBm on each polarization generates the PDM signals. In the characterization calculation, the PDM signals are supposed to have the same phase information for simplicity. The idlers involving into the vector PSA are prepared at 1555.5nm and carrying the same phase information as the corresponding signals.

For simplicity, the signal and idler powers are usually identical in the scalar PSA, while it is different in our scheme, where the signal-to-idler power ratio σ should be optimized. The PSG of one PDM component is shown as a function of σ for different P_{pumps} in Fig. 3. Two guidelines should be followed in the optimization. Firstly, the P_{pumps} should not exceed 30 dBm to avoid or weaken the SBS effect [5]. Secondly, a large σ is preferred, considering the idler is usually achieved from a signal-involved FWM process in the practical experiment, where the idler power is limited by the signal power. As shown in Fig. 3, the optimal σ increases with the increasing P_{pumps}. Consequently, a σ of −2 dB is selected for P_{pumps} = 30 dBm. The signal obtains a PSG of ~29.5 dB.

#225809 - $15.00 USD Received 27 Oct 2014; revised 11 Dec 2014; accepted 6 Jan 2015; published 26 Jan 2015

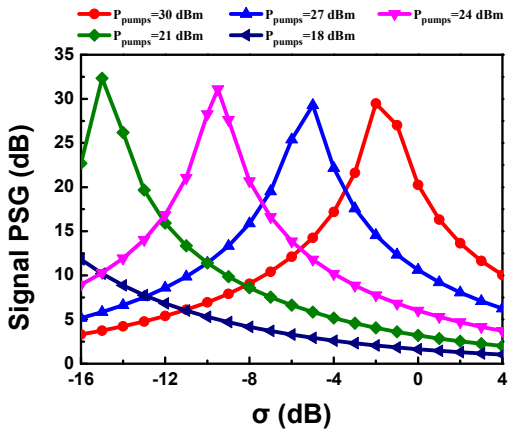

Fig. 3. Calculated signal phase sensitive gain (PSG) as a function of the input signal-to-idler ratio σ for different total pump power, P_{pumps}, i.e. P_{pumps} = 18, 21, 24, 27 and 30 dBm.

In the above simulation, the Δβ is constant because of the fixed wavelengths and the dispersion parameters of the HNLF. In order to investigate the influences of the Δβ on the signal PSG, the signal PSG is further calculated as a function of the Δβ, the corresponding result is shown in Fig. 4. One can observe that the PSG curve is close to a periodic function, whose peak-to-valley ratio is ~5 dB. Although the PSG is affected by the Δβ, the minimum PSG is large enough to realize the phase squeezing function for the distorted DPSK signal. Consequently, the initial sets for the wavelengths and the dispersion parameters for the HNLF keep constant in the next simulation. In the practical experiment, one can adjust the Δβ thus to optimize the PSG.

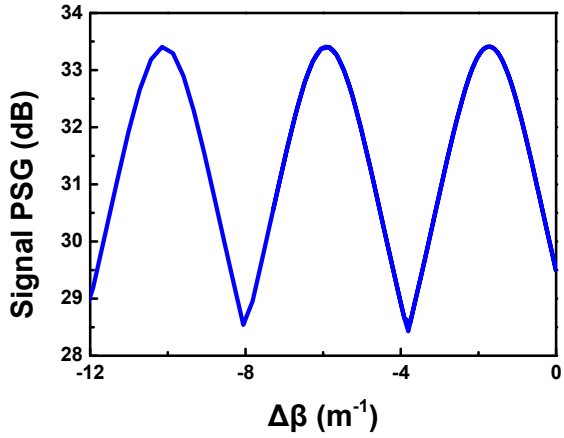

Fig. 4. Calculated signal phase sensitive gain (PSG) as a function of the linear phase matching factor, Δβ.

On the other hand, for the PR of the degraded signals, saturate PSA gain is also needed to decrease the amplitude noise (AN) caused by the intrinsic PSA gain curve. This can be realized by a larger P_{signal}, which can alternatively avoid using the overlarge pump power. Thus, the PSG changes over the P_{signal} are shown in Fig. 5. The PSG keeps constant when the signal power is less than −10dB, and it begins to decrease because of the saturate effect, when the signal power increases. To achieve a good regenerative performance, an appropriate P_{signal} should be chosen to ensure both the step-like phase and saturate gain transfer characteristic.

#225809 - $15.00 USD Received 27 Oct 2014; revised 11 Dec 2014; accepted 6 Jan 2015; published 26 Jan 2015

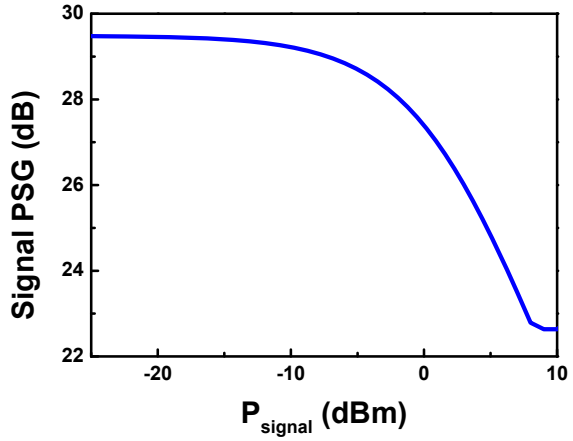

Fig. 5. Calculated signal phase sensitive gain (PSG) as a function of the signal power, P_{signal}.

Figure 6 shows the transfer functions of the vector scheme for different signal power (i.e. P_{signal} = 1, 7, 13 dBm) in the PSG saturate region. Figure 6(a) and (b) correspond to gain and phase transfer functions, respectively. In the PSG saturate region, deep saturability is achieved for large signal power. However, excessive saturation will result in the degraded phase and gain transfer functions. Considering both the output amplitude and phase, a moderate saturation is preferred as a tradeoff. Consequently, the signal power of 7 dBm is chosen for the next PR simulation.

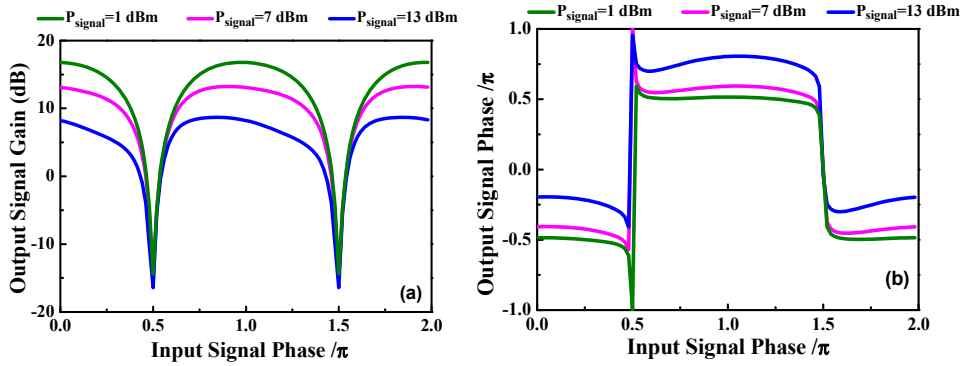

Fig. 6. Transfer function of (a) gain and (b) phase.

3.2. PR of PDM DPSK signals

The PR performance based on the proposed scheme is further simulated. Two signals are both independently modulated with distinct phase information at 40 Gbit/s in the RZ-DPSK format with a duty cycle of 50% (PRBS 2^{11}-1) and subsequently distorted by adding the white Gaussian phase noise, generating the 80 Gbit/s PDM signals. The simulation results are depicted in Fig. 7. The PN of each input PDM components is distributed to $\sim 85^{\circ}$, the constellations of the output signals indicate effective phase squeezing after the regeneration process. The AN of the regenerated signals, which has been suppressed by the saturate vector PSA, are still existing owing to the intrinsic phase-to-amplitude conversion in PSA. In order to quantify the regeneration performance, a metric EVM, which synthetically consider both PN and AN based on input and output constellations, is introduced. It describes the effective

#225809 - $15.00 USD Received 27 Oct 2014; revised 11 Dec 2014; accepted 6 Jan 2015; published 26 Jan 2015

distance of the received complex symbol from its ideal position, can be defined as follows [29]:

$$EVM = \frac{\left(\frac{1}{I}\sum_{i=1}^{I}\left|E_{r,i} - E_{t,i}\right|^2\right)^{1/2}}{\left|E_{t,m}\right|} \tag{2}$$

where $E_{r,i}$ and $E_{t,i}$ is the actually received signal vector and the ideal signal vector, respectively. $\left|E_{t,m}\right|$, serving for normalization, is the power of the longest ideal constellation vector. I is the bit length of the signal data. The EVM for each distorted PDM component is 22.58% and 21.39%, and then decreased to 4.57% and 4.63% thanks to the PSA processes. For comparison, the EVM plots of the PDM signals before and after the PR are presented in Fig. 8, showing the phase squeezing tolerance of the proposed scheme. For all these different added PN, good improvements in the EVM can be observed.

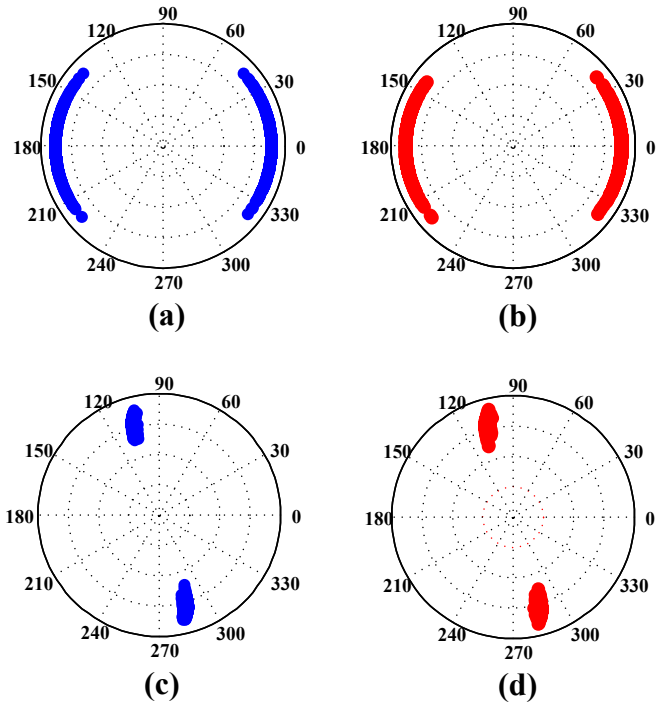

Fig. 7. Simulated constellation of PDM DPSK signals: (a) x-pol signal without PSA; (b) y-pol signal without PSA; (c) regenerated x-pol signal; (d) regenerated y-pol signal.

#225809 - $15.00 USD Received 27 Oct 2014; revised 11 Dec 2014; accepted 6 Jan 2015; published 26 Jan 2015

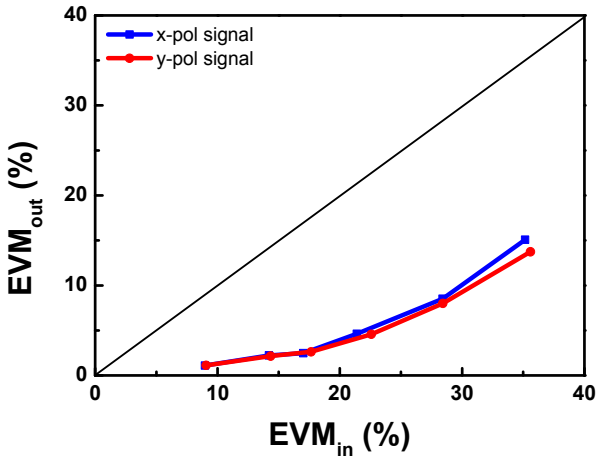

Fig. 8. EVM of the PDM DPSK signals before and after PR.

3.3. PR of PDM QPSK signals

We further investigate the applicability of the scheme to PDM-QPSK signals. Four-order staircase-like phase transfer function is needed, which can be realized by interfering the signal with a conjugated 3th phase harmonic [30]. Thus, the idlers involved in each PSA process are supposed to be launched with 3 times phase of the corresponding input signals for simplicity. The total launched power of the input waves is ~30 dBm. The simulated constellations are shown in Fig. 9. The output results indeed show an improved phase performance after the PR. Meanwhile, the EVM, which are 9.78% and 10.24% for each PDM component at the input of the PSA, are improved to 2.4% and 2.71% after regeneration. For a real experimental system, the implementation to achieve the 3th-order harmonic may be difficult, and a considerable solution is based on the high-order FWM processes [11]. The other processing is similar to our operation for the PR of the DPSK signals (Fig. 2).

#225809 - $15.00 USD Received 27 Oct 2014; revised 11 Dec 2014; accepted 6 Jan 2015; published 26 Jan 2015

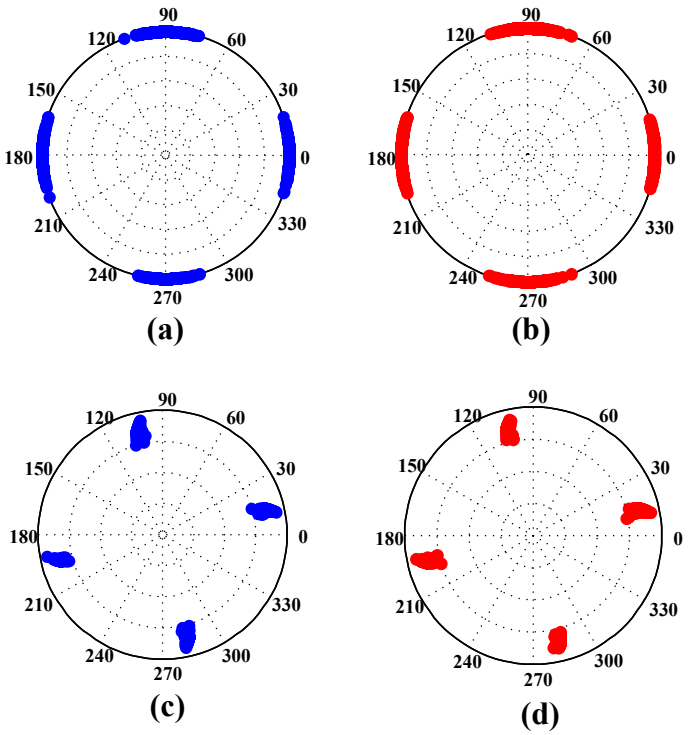

Fig. 9. Simulated constellation of PDM QPSK signals: (a) x-pol signal without PSA; (b) y-pol signal without PSA; (c) regenerated x-pol signal; (d) regenerated y-pol signal.

4. Conclusions

In summary, the PR for PDM signals utilizing the vector dual-pump nondegenerate PSA in a HNLF is proposed and demonstrated. A theoretical model is established and the PR performance is characterized in detail. In order to realize the PDM PR and avoid utilizing the polarization-diversity set-up, the vector dual-pump nondegenerate configuration is employed. The PR for 80 Gbit/s PDM DPSK and QPSK signals are achieved successfully. The PR tolerance is also investigated. This scheme will accelerate the process of realizing the PR for the PDM signals in the fiber optic communication systems.

Acknowledgments

This work was supported by the National Basic Research Program of China (Grant No.2011CB301704), National Natural Science Foundation of China (Grant No. 61475050, 61275072 and 61125501), and the New Century Excellent Talent Project in Ministry of Education of China (NCET-13-0240).